Applied Catalysis B: Environmental 189 (2016) 51–55

Contents lists available at ScienceDirect

Applied Catalysis B: Environmental

journal homepage: www.elsevier.com/locate/apcatb

Crystal structure and photoelectric conversion properties of eosin Y-adsorbing ZnO films prepared by electroless deposition

Satoshi Nagaya[a], Hiromasa Nishikiori[b,*], Hideaki Mizusaki[a], Kosuke Sato[a], Hajime Wagata[b], Katsuya Teshima[b]

[a] Nagano Prefecture General Industrial Technology Center, 1-3-1, Osachi-Katamacho, Okaya, Nagano 394-0084, Japan
[b] Department of Environmental Science and Technology, Faculty of Engineering, Shinshu University, 4-17-1, Wakasato, Nagano 380-8553, Japan

ARTICLE INFO

Article history:
Received 10 November 2015
Received in revised form 29 January 2016
Accepted 4 February 2016
Available online 6 February 2016

Keywords:
ZnO
Eosin Y
Electroless deposition
Crystal growth
Photoelectric conversion

ABSTRACT

Eosin Y-adsorbing ZnO thin films were prepared on substrates by electroless deposition from aqueous solutions containing zinc nitrate, dimethylamine–borane, and eosin Y. The concentration of eosin Y in the solution changed the structure of the deposited ZnO particles on the substrate. In the absence of eosin Y in the solution, the ZnO crystals preferred to grow in the c-axis direction. In the presence of eosin Y in the solution, the orientation of the ZnO was in the a-axis direction. As the eosin Y concentration increased, the size of the ZnO crystallites decreased and they became aggregated due to a strong interaction between the eosin Y and the (0002) plane of the ZnO, and consequently, the film resistance increased due to their boundary. The electron injection efficiency increased due to the strong interaction although the electron transfer efficiency decreased. The ZnO crystallite size, eosin Y amount, and their interaction increased the energy conversion efficiency.

1. Introduction

Metal oxide semiconductors, such as ZnO and TiO_2, have been used in various industries, and studied as photocatalysts [1] and photofunctional [2] materials by exploiting their interesting characteristics. Recently, the studies of electronic devices using such materials for photoelectric conversion [3] and sensing [4] have progressed.

Among them, the preparation of the organic dye-adsorbing metal oxide semiconductor particles was studied [5]. ZnO and TiO_2 cannot function as photocatalyst during visible light irradiation, but it is possible to function when they adsorb organic dyes exhibiting absorption in the visible light region [6]. The dye sensitized solar cells (DSSCs) [7] or visible-light photocatalysts [8] using them have attracted considerable attention as highly efficient materials.

The electrodes of DSSCs using TiO_2 as a semiconductor were prepared by the following 3 steps: (1) The TiO_2 sol paste was spread by a doctor blade method on an electrically-conductive glass substrate; (2) The substrate was heated at about 773 K and the TiO_2 film was formed; and (3) The substrate was immersed in an alcohol solution of the organic dye, which was adsorbed on the TiO_2. Under the present conditions, the energy conversion efficiency of the DSSCs using ZnO is lower than that using TiO_2 [9–11]. However, ZnO is a potential material because it shows a higher electron mobility than TiO_2 [9]. Besides, the productivity of the ZnO-based DSSCs is higher than the TiO_2-based ones because ZnO can be prepared by heating at a lower temperature [12–14]. It is environmentally-friendly and economically important that the efficiency is improved and sufficient for practical use.

The ZnO films can be prepared by various methods. Among them, electrodeposition [12,13] and electroless deposition [14] using $Zn(NO_3)_2$ or $ZnCl_2$ can produce ZnO at a low temperature under 373 K. TiO_2 films are difficult to prepare by such methods. Furthermore, it was possible that the organic dye-adsorbing ZnO was spontaneously formed by mixing the dye in a solution with a one–step deposition [15,16].

We previously prepared eosin Y-adsorbing ZnO thin films by electroless deposition and evaluated them for use as solar cell electrodes [17,18]. Eosin Y is used as a sensitizing dye because it has high stability, versatility, and light absorptivity. There are many reports on the DSSCs using eosin Y-adsorbing ZnO electrodes [19,20]. In such studies, a heat treatment was required for crystallization of the ZnO in the preparation process, which made it difficult to form the crystals on low heat-stable materials. Yoshida et al. successfully prepared the highly-efficient DSSC electrodes containing the eosin Y-adsorbing ZnO films by electrodeposition

* Corresponding author.
E-mail address: nishiki@shinshu-u.ac.jp (H. Nishikiori)

http://dx.doi.org/10.1016/j.apcatb.2016.02.013
0926-3373/© 2016 Published by Elsevier B.V.

[21]. The small ZnO particles can induce the higher efficiency. Compared to electrodeposition, the size of the ZnO particles prepared by eletcroless deposition was very small because the electroless deposition applied a lower potential than the electrodeposition [14].

The rate of electroless deposition of ZnO is lower than that of electrodeposition. For electroless deposition, it takes several hours to prepare a few micrometer thick ZnO film because the deposition progresses by only oxidation-reduction reactions using a reducing agent in the solution. During the electroless deposition process, it is effective to use Pd particles as a catalyst on the substrate surface before the electroless deposition [14,22]. It is expected that electroless deposition can provide a thin ZnO film consisting of smaller particles as a higher amount of the dye is adsorbed on the ZnO particles. Smaller particles are prepared by the slower reactions. In the DSSCs, it was considered that the films of the electrodes were efficient due to the strong interaction between the higher amount of the dye molecules and the smaller-sized ZnO [23,24], therefore, electroless deposition is expected to produce high performance photoelectric conversion devices. Besides, it is interesting to study the influence of the ZnO structure on the electrochemical properties because the ZnO crystals of various forms can be prepared by electroless deposition.

In this study, we simply prepared thin ZnO films on the substrate by electroless deposition without using Pd for a much slower deposition and examined the ZnO crystal structure, its interaction with the dye molecules, and their influence on the photoelectric conversion properties.

2. Experimental

2.1. Materials and preparation of electrodes

Fluorine-doped tin oxide (FTO) glass plates (9 Ω cm^{-2}, AGC Fabritech) or glass plates (Matsunami Glass S1225) were coated with ca. 30-nm-thick ZnO thin films as a buffer layer [25] and used as the substrates. The main ZnO films were deposited from aqueous solutions containing reagent-grade chemicals and distilled water. The buffer layer was prepared by dip-coating in 2-methoxyethanol containing 0.25 mol dm^{-3} zinc acetate and 0.0125 mol dm^{-3} 2-aminoethanol. After the dip-coating, the substrates were heat-treated at 723 K for 30 min. The FTO surface resistance was 15 Ω cm^{-2} after the heating.

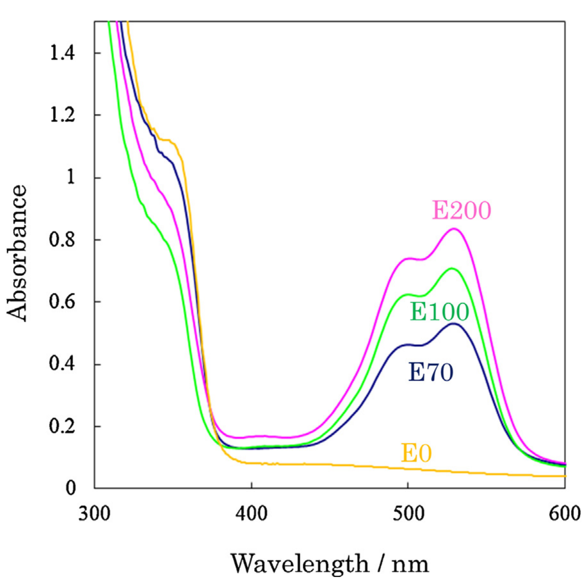

Fig. 1. UV–vis absorption spectra of E0, E70, E100, and E200.

Before the electroless deposition, the substrates with ZnO thin films were rinsed in 2-propanol and distilled water along with ultrasonication for 1 min.

Electroless deposition of the eosin Y-adsorbing ZnO films was conducted using an aqueous solution containing 0.050 mol dm^{-3} $Zn(NO_3)_2$, 0.025 mol dm^{-3} dimethylamine–borane (DMAB), and 0–200 μmol dm^{-3} eosin Y. The solution was prepared under the condition of ca. pH 6 and stored at 333 K with stirring. After the electroless deposition, the substrates were washed with distilled water and separately dried at 343 K and 423 K for 30 min. The film samples prepared from the aqueous solutions containing 0, 70, 100, and 200 μmol dm^{-3} eosin Y were labeled E0, E70, E100, and E200, respectively. The deposition rate decreased with an increase in the eosin Y concentration. The film thickness of the samples was adjusted by the deposition time, which increased the amount of the deposited ZnO particles.

2.2. Measurements

The UV–vis absorption spectra of the samples were measured using a spectrophotometer (Hitachi U-4000). The surface morphology of the samples was observed using a scanning electron microscope, and elemental analysis was conducted by energy-dispersive X-ray spectroscopy (SEM-EDS, JEOL JSM-6010LA). The thickness of the films was obtained using an X-ray fluorescence analyzer (XRF, Seiko Instruments SEA5150). The X-ray diffraction patterns were obtained using an X-ray diffractometer (XRD, Rigaku RINT2100).

For examination of the photoelectrochemical properties, the electrolyte solution consisting of acetonitrile and ethylene carbonate (v/v = 1/4) containing 0.50 mol dm^{-3} KI and 0.030 mol dm^{-3} I_2 was allowed to soak into the space (using about a 4-μm spacer) between the working and counter Pt electrodes. The samples were irradiated with monochromatic light obtained from a fluorescence spectrophotometer (Hitachi F2000) with a Xe short arc lamp (0.32 cm^2 irradiation area). During the light irradiation, the short circuit current was measured in the range from 300 to 600 nm by a digital multimeter (Agilent 34405A). The *J-V* curves of the samples were measured by a potentiostat during the light irradiation using the Xe short arc lamp with an air mass filter (350–1050 nm, 100 mW cm^{-2}).

3. Results and discussion

3.1. Characterization of the eosin Y-adsorbing ZnO films

The amount of the red suspensions increased with increases in the concentration of eosin Y in the solution and the deposition time. Zinc atoms were detected in the suspensions by elemental analysis. This indicated that a large amount of the eosin Y-adsorbing ZnO particles was formed from the solution during the electroless deposition process.

Fig. 1 shows the absorption spectra of the eosin Y-adsorbing ZnO films. The absorption peak intensity at 525 nm increased with an increase in the concentration of eosin Y in the solution. The absorption band at around 400–600 nm is assigned to eosin Y and the absorption band having a peak at 525 nm is assigned to the eosin Y monomer [26]. The film thicknesses were determined to be 0.3, 0.3, 0.2, and 0.2 μm for E0, E70, E100, and E200, respectively. This spectral difference indicated the amount of eosin Y monomer in the film. The absorbance values at 350 nm for E0 and E70 were higher than those for E100 and E200 depending on their film thickness because the absorption band at around 350 nm was assigned

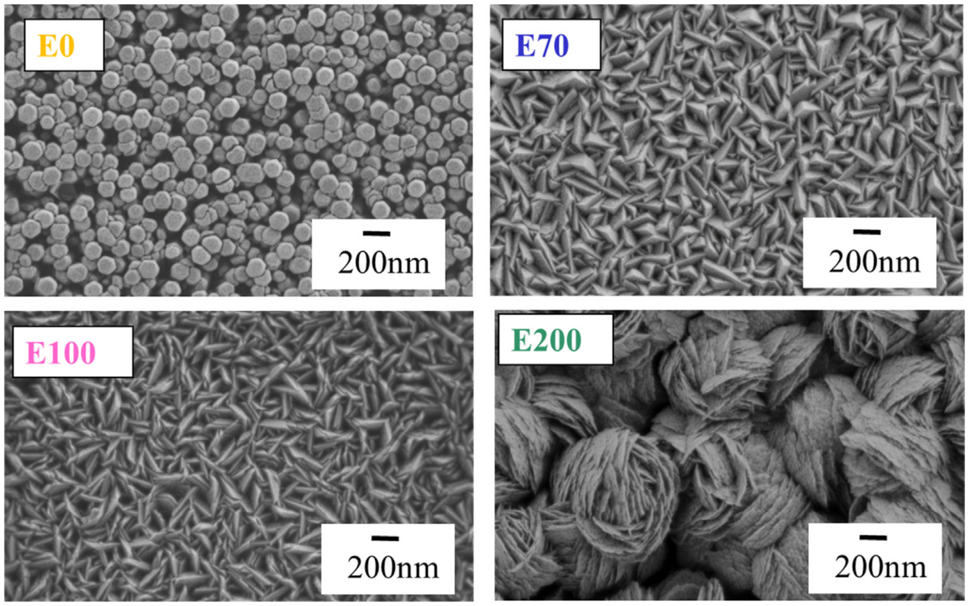

Fig. 2. SEM images of the surfaces of E0, E70, E100, and E200.

to the ZnO. The maximum absorbance values at 400–600 nm were 0.54, 0.70, and 0.84 for E70, E100, and E200, respectively. The molar absorption coefficient of eosin Y at 530 nm was determined to be $5.6 \times 10^4\ dm^3\ mol^{-1}\ cm^{-1}$ from the KOH solution which dissolved the eosin Y from E70 with a 0.3 μm-thickness. The concentrations of eosin Y were calculated to be 0.32, 0.63, and 0.79 mol dm^{-3} for E70, E100, and E200, respectively. The ZnO films thinner than the general TiO_2 films can be easily prepared by electroless deposition [7].

Fig. 2 shows SEM images of the surface of the samples prepared for observation. Their film thickness was ca. 1.3–1.7 μm. The hexagonal phase in E0 grew linearly and vertically on the substrate surface. The surface morphologies of E70 and E100 were similar, but that of E200 was different from them. The flake-shaped crystals stood vertically on the substrate surface and were very densely packed in E70 and E100. The crystals were aggregated and formed secondary particles in E200. The particle size estimated from the SEM images were ca. 150, 200, 400, and 800 nm for E0, E70, E100, and E200, respectively. The particle size increased with an increase in the concentration of eosin Y in the solution.

Fig. 3 shows the XRD patterns of the films with an ca. 1.3–1.7-μm thickness. Only a strong $(0\,0\,0\,2)$ peak of wurtzite ZnO was observed in E0. This result indicated that the ZnO crystals preferred to grow in the c-axis direction in E0. The relative intensities of the $(1\,0\,\bar{1}\,1)$ and $(1\,0\,\bar{1}\,2)$ peaks of the wurtzite ZnO were stronger than those of the other peaks in E70 and E100, while that of the $(1\,0\,\bar{1}\,0)$ peak was stronger in E200. The peak shape became broader with an increase in the concentration of eosin Y. The crystallite size was estimated from the full width at half-maximum of the $(1\,0\,\bar{1}\,1)$ peaks using Scherrer's equation shown in parentheses in Fig. 3. The crystallite size decreased with an increase in the concentration of eosin Y in the raw solution. These results indicated that the particles observed in the SEM images were aggregates of the ZnO crystals.

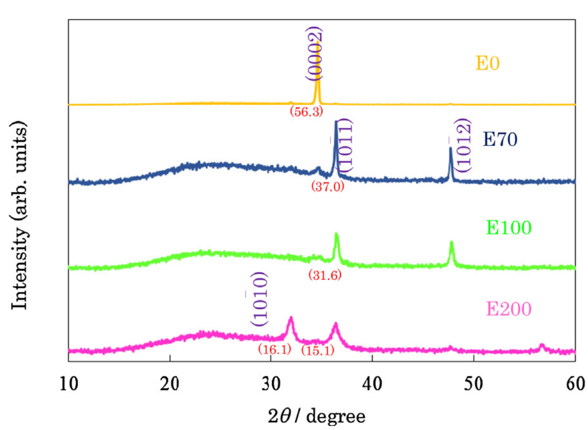

Fig. 3. X-ray diffraction patterns of E0, E70, E100, and E200.
The crystallite size was estimated using Scherrer's equation shown in parentheses.

Generally, ZnO crystals having a hexagonal structure prefer to grow in the c-axis direction because the $(0\,0\,0\,2)$ plane has a highest surface energy [27] and polarity [28] in the wurtzite ZnO. Eosin Y is preferentially adsorbed on the $(0\,0\,0\,2)$ plane of ZnO and inhibited the ZnO growth in the c-axis direction. As a result, the ZnO preferred to grow in the direction of the a-axis, thus the intensities of the $(1\,0\,\bar{1}\,1)$ and $(1\,0\,\bar{1}\,2)$ peaks in E70 and E100 were stronger than those of the other peaks. In E200, the amount of eosin Y adsorbed on the ZnO particles was greater than those in the other films. The ZnO crystallite size was smaller because the eosin Y adsorbed on their surface and inhibited the crystal growth. Therefore, the ZnO crystallinity decreased, its surface became hydrophilic, and the ZnO particles were aggregated. It is expected that the photoelectrochemical properties of the films depend on the structure of the ZnO particles.

3.2. *Photoelectric conversion properties of the eosin Y-adsorbing ZnO films*

Fig. 4 shows the photocurrent action spectra of the samples. It was confirmed that eosin Y functioned as a sensitizer because

Table 1
Absorbed photon-to-current quantum efficiency (APCE) in the UV and visible ranges and their ratios for the electrodes.

Electrode	UV range (A)	Visible range (B)	Ratio (B/A)
E70	0.47 (350 nm)	0.31 (530 nm)	0.66
E100	0.36 (350 nm)	0.25 (530 nm)	0.69
E200	0.31 (350 nm)	0.24 (530 nm)	0.77

Table 2
Photovoltaic characteristics of E70, E100, E200,and E100 (1.0 μm).

Electrode	Open circuit voltage	Short circuit current	Fill factor	Energy conversion efficiency
E70	0.45 V	1.31 mA cm^{-2}	0.32	0.21%
E100	0.50 V	0.94 mA cm^{-2}	0.47	0.23%
E200	0.53 V	1.11 mA cm^{-2}	0.59	0.36%
E100 (1.0 μm)	0.50 V	2.24 mA cm^{-2}	0.57	0.67%

the shape of the action spectra in the range from 400 to 600 nm was similar to that of the absorption spectra in Fig. 1. The incident photon-to-current conversion efficiency (IPCE) values in the range from 400 to 600 nm were 20–25% and independent of the concentration of eosin Y. The photocurrent action spectra in the range from 300 to 400 nm assigned to the ZnO decreased with an increase in the eosin Y concentration. The absorbed photon-to-current quantum efficiency (APCE) was estimated based on the absorption spectra shown in Fig. 1. Table 1 shows the APCE values in the UV and visible ranges and their ratios, which depended on the efficiency of the electron injection from the dye. The APCE values at 350 nm decreased with an increase in the concentration of eosin Y in the film whereas those at 530 nm slightly decreased. The APCE decrease at 350 nm occurred because the resistance of the film increased with increases in the amounts of the eosin Y and the boundary of the ZnO crystals. The APCE ratio values indicated that the electron injection efficiency increased with an increase in the concentration of eosin Y. As already stated, the eosin Y molecules were preferentially adsorbed on the (0 0 0 2) plane of ZnO because the interaction between the molecule and plane was strong due to the high polarity of the plane. The eosin Y monomer was a preferential species and only slightly aggregated in the films because the interaction with the ZnO surface was stronger than that between the molecules. It is suggested that the electron injection efficiency increased with an increase in the amount of eosin Y adsorbed on the ZnO due to the strong interaction.

The SEM images in Fig. 2 show the different structures of the ZnO particles in the individual films. We investigated the relationship between the structure of ZnO particles and their photoelectric properties. The photocurrent action spectra of the samples were obtained after the samples were immersed in the KOH solution in order to desorb the eosin Y. The IPCE values in the UV region were similar to those of the original samples shown in Fig. 4 although those in the visible region were significantly lower. Based on these results, the IPCE values in the UV region depend on the ZnO crystal structure rather than the amount of the adsorbed eosin Y, and the APCE value in the UV region indicates the efficiency of the electron transfer in the ZnO crystals.

In E70, E100, and E200, the crystallite size decreased with an increase in the concentration of eosin Y as shown in Fig. 3. This is due to the fact that as the concentration of the eosin Y increased, the size of the ZnO crystallites became smaller and they formed aggregates, that is, the electron transfer efficiency decreased with an increase in the resistance of the ZnO film due to the high amount of boundaries. It is suggested that a large crystallite size and high amount of eosin Y can effectively to improve the efficiency.

Fig. 5 and Table 2 show the *J-V* curves of E70, E100, and E200 with a 0.2–0.3 μm film thickness and E100 with a 1.0 μm film thickness, and their properties, respectively. The open circuit voltage, fill factor, and energy conversion efficiency increased with an increase in the concentration of eosin Y due to the strong interaction between the eosin Y and ZnO particle surface. The short circuit photocurrent in E100 with the 1.0 μm film thickness (2.2 absorbance) was the highest in all the samples, and its energy conversion efficiency was 0.67%. This value was 2.9 times greater than that of E100 with a 0.2 μm film thickness because the amount of adsorbed eosin Y increased with the thickness. The internal energy conversion efficiency, i.e., the energy conversion efficiency relative to the total energy of the absorbed photons, was 5.45% for E100 with the 1.0 μm thickness. Even though the energy conversion efficiency is low for practical use in a solar cell, it is expected that the efficiency will be improved by an increase in the film thickness and optimization of the ZnO crystal morphology and dye adsorption.

4. Conclusion

The films consisting the eosin Y-adsorbing ZnO particles were prepared on substrates by electroless deposition from aqueous solutions containing $Zn(NO_3)_2$, DMAB, and eosin Y. As the concentration of eosin Y in the solution increased, the eosin Y molecules adsorbed on the ZnO particles which changed their crystal growth. Based on the XRD analysis, only a strong (0 0 0 2) peak of wurtzite ZnO was observed in the film without eosin Y. This result indicated that the ZnO crystals preferred to grow in the c-axis direction. With an increase in the eosin Y concentration, the relative intensities of the (1 0 $\bar{1}$ 1) and (1 0 $\bar{1}$ 2) peaks of ZnO became stronger than those of the other peaks, and then that of the (1 0 $\bar{1}$ 0) peak became

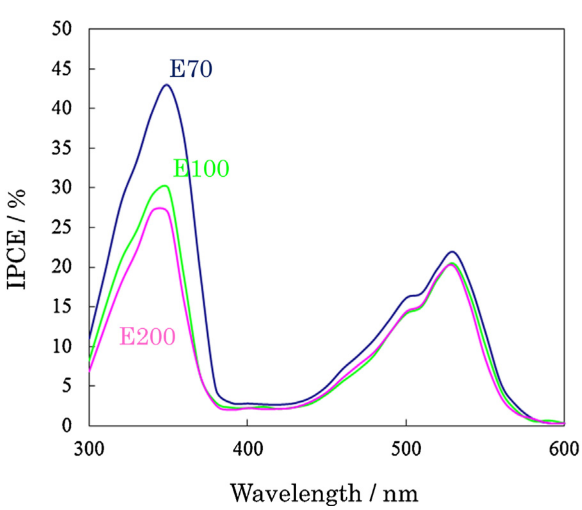

Fig. 4. Photocurrent action spectra of E70, E100, and E200.

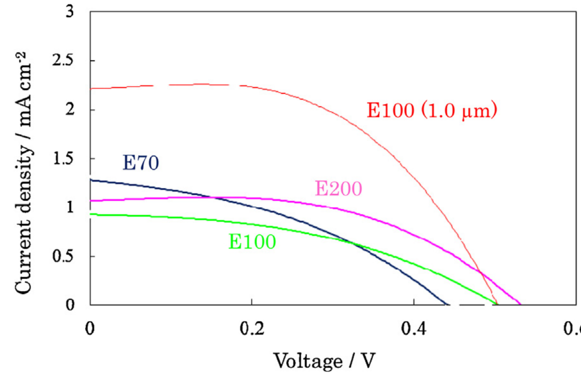

Fig. 5. *J-V* curves of E70, E100, E200, and E100 (1.0 μm).

stronger. An increase in the eosin Y concentration decreased the ZnO crystallite size. The smaller ZnO crystallites were more easily aggregated, and consequently, the film resistance became higher due to their boundary. The difference in the ZnO structure affected the photoelectrochemical properties. The electron injection efficiency increased due to the strong interaction between the eosin Y and ZnO particle surface with an increase in the eosin Y concentration although the electron transfer efficiency decreased. The ZnO crystallite size, eosin Y amount, and their interaction increased the energy conversion efficiency. The internal energy conversion effici ency was 5.45% for the electrode with a 1.0 μm thickness prepared from the 100 μmol dm^{-3} eosin Y solution.

References

[1] A. Fujishima, K. Honda, Nature 238 (1972) 37–38.
[2] C.M. James, L. Robert, V.T. Cody, Coatings 4 (2014) 651–669.
[3] M. Izaki, Chem. Commun. 24 (2002) 476–477.
[4] I.A. Al-Homoudi, J.S. Thakur, R. Naik, G.W. Auner, G. Newaz, Appl. Surf. Sci. 253 (2007) 8607–8614.
[5] J.Y. Kim, Opt. Commun. 321 (2014) 86–89.
[6] B. Zhang, W. Zhao, Y. Cao, X. Wang, Z. Zhang, X. Jiang, S. Xu, Synth. Metals 91 (1997) 237–241.
[7] B. Regan, M. Gratzel, Nature 353 (1991) 737–740.
[8] I. Poulios, E. Micropoulou, R. Panou, E. Kostopoulou, Appl. Catal. 41 (2003) 345–355.
[9] J.A. Anta, E. Guillen, R. Tena-Zaera, J. Phys. Chem. C 116 (2012) 11413–11425.
[10] N. Memarian, I. Concina, A. Brage, S.M. Rozati, A. Vomiero, G. Sberveglieri, Angew. Chem. Int. Ed. 50 (2011) 12321–12325.
[11] M. Saito, S. Fujihara, Energy Environ. 1 (2008) 280–283.
[12] M. Izaki, T. Omi, Appl. Phys. Lett. 68 (1996) 2439–2440.
[13] S. Peulen, D. Lincot, J. Electrochem. Soc. 145 (1998) 864–874.
[14] M. Izaki, T. Omi, J. Electrochem. Soc. 144 (1997) L3–L5.
[15] T. Yoshida, K. Terada, D. Schlettwein, T. Oekermann, T. Sugiura, H. Minoura, Adv. Mater. 16 (2000) 1214–1217.
[16] T. Yoshida, M. Tochimoto, D. Schlettwein, D. Wohrle, T. Sugiura, H. Minoura, Chem. Mater. 11 (1999) 2657–2667.
[17] S. Nagaya, H. Nishikiori, ACS Appl. Mater. Interfaces 5 (2013) 8841–8844.
[18] S. Nagaya, H. Nishikiori, H. Mizusaki, H. Wagata, K. Teshima, ACS Appl. Mater. Interfaces 7 (2015) 11592–11598.
[19] P. Suri, M. Panwer, R.M. Mehra, Mater. Sci. Pol. 25 (2007) 137–144.
[20] W.J. Lee, H. Okada, A. Wakahara, A. Yoshida, Ceram. Int. 32 (2006) 495–498.
[21] T. Yoshida, J. Zhang, D. Komatsu, S. Sawatani, H. Minoura, T. Pauporte, D. Lincot, T. Oekermann, D. Schlettwein, H. Tada, D. Wohrle, K. Funabiki, M. Matsui, H. Miura, H. Yanagi, Adv. Funct. Mater. 19 (2009) 17–43.
[22] T. Shinagawa, K. Murase, S. Otomo, J. Katayama, M. Izaki, J. Electrochem. Soc. 156 (2009) H320–H326.
[23] L. Bo, L. Xiaoyan, L. Miaoyin, N. Zhijun, Z. Qiong, L. Chen, M. Klaus, Z. Weihong, Dyes Pigments 94 (2012) 23–27.
[24] S. Wenye, P. Bosi, L. Li, L. Renjie, Z. Jing, P. Tianyou, Mater. Chem. Phys. 163 (2015) 348–354.
[25] P.J. Cameron, L.M. Peter, J. Phys. Chem. B 107 (2003) 14394–14400.
[26] S. De, S. Das, A. Girigoswami, Spectrochim. Acta A 61 (2005) 1821–1833.
[27] X.Y. Kong, Z.L. Wang, Appl. Phys. Lett. 84 (2004) 975–977.
[28] B.G. Wang, E.W. Shi, W.Z. Zhong, Cryst. Res. Technol. 33 (1998) 937–941.